Influence of Film Thickness on Optical Properties of Hydrogenated Amorphous Silicon Thin Films

A. M. Bakry

Physics Department, Faculty of Science, Ain-Shams University, Cairo, Egypt 11566.

A detailed study of the dependence of optical constants on thickness for vacuum-deposited hydrogenated amorphous silicon thin films is reported. The thicknesses of the films range from 190 nm to 540 nm. The refractive index n(λ), absorption coefficient α(λ), extinction coefficient k(λ) and consequently the band gap, are determined from the spectrophotometric measurements of the film transmittance in the wavelength range 400-2500 nm. The average gap E_w is calculated as well using Wemple's equations. A comparison between different mechanisms to study the band gap and their correla[1]tion to the obtained results is given. The carrier concentration N/m^*, static refractive index n_o and the high frequency dielectric constant ε_∞ were studied.

1. Introduction

Amorphous hydrogenated silicon (a-Si:H) has attracted much attention in the field of electronic devices, particularly for the production of large inexpensive photovoltaic arrays. Many papers have been published on the influence of substrate temperature, hydrogen content, doping and flow rate on the optical properties of a-Si:H films [1-5]. However, the influence of film thickness on optical properties does not appear to have enough investigation.

Amorphous thin films often exhibit inhomogeneties, where the mean grain size at the surface of the films are found to depend on film thickness [6,7]. An inhomogeneous region close to the substrate would play an increasingly important role as the film thickness decreases. It is possible to estimate the effect of inhomogeneities from the knowledge of the measured complex dielectric constant. Therefore the dependence of optical constants on thickness can give information about inhomogeneity in the films.

E-mail: assem_sedfy@yahoo.com

Different preparation techniques were used to study the effect of thickness on the optical properties of the a-Si:H films such as magnetron sputtering [8], glow discharge [8,9] plasma-enhanced chemical vapor deposition [10] and vacuum deposition [11]. Reactive magnetron sputtering was used for Nb_2O_5 films [12]. Hot wall deposition was also used to prepare CdSe thin films [13]. Other researchers used thermal evaporation to prepare $(Ge_2S_3)(Sb_2Se_3)$ [14], InSe [15] thin films, $Ga_8As_{46}Te_{46}$ [16] and $As_{45.2}Te_{46.6}In_{8.2}$ [17]. A final conclusion could be drawn, that, regardless of the film composition and the preparation technique, film thickness affects significantly the properties of the film.

In the present work, the effect of film thickness on the optical gap, refractive index and carrier concentration for a-Si:H films is studied.

2. Experimental procedures:

The preparation of the films was carried out in Klaushal Ziellerfield Technical University in Germany. The investigated films were prepared on Corning 7059 glass substrates at a temperature 300°C. Silicon was evaporated from an electron beam heated vitreous Carbon crucible at a rate of approximately 3 A° per second to a thickness of about 5000 A°. The film thickness was measured by the Tolansky method of multiple beam Fizeau fringes [18]. The base pressure of vacuum was 10^{-7} mbar. During the entire evaporation process, atomic hydrogen was blown at the growing film from a radio frequency dissociation system. The resulting hydrogen pressure in the vacuum vessel was 3×10^{-5} mbar and the hydrogen flux through the dissociator was about 16 ml N/min. The hydrogen content in all used films was kept fixed at C_H=12 at.%. The transmittance, *T*, and reflectance, *R*, spectra were carried out between 400 and 2500 nm in steps of 2 nm using a computer-aided double-beam spectrophotometer (Shimadzu 3101 PC UV-VIS-NIR). The relative uncertainty in the transmittance and reflectance is 0.2%. Transmittance scans were performed using a glass substrate in the reference compartment of the same kind that was used for the film deposition. The transmittance and reflectance were measured at the same incidence angle of 5º.

3. Determination of the optical constants

3.1. Film thickness *d*

The film thickness d was also estimated using the method proposed by Ambrico [19]. If n11 and n12 are the refractive indices at two adjacent maxima (or minima) at λ1 and λ2 then

$$d_1 = \frac{\lambda_1 \lambda_2}{2(\lambda_1 n_{12} - \lambda_2 n_{11})} \qquad (1)$$

The d_1 values have been derived at each extremum and averaged $\langle d_1 \rangle$. Then using the equation of interference fringes

$$2n_1 \langle d_1 \rangle = m' \lambda \qquad (2)$$

where m' is the order of interference and generally not an integer number. True order numbers m is calculated by rounding m' values to integer or half integers. Using values of m and n_1 in the equation

$$2n_1 \langle d_2 \rangle = m\ \lambda$$

d_2 values at each wavelength and average corrected thickness $\langle d_2 \rangle$ is determined. Eqn. 2 is used to determine exact integer (for maxima) or half integer (for minima) values of m for each λ. Exact values of d can be calculated using n values again. The set of m that gives the smallest dispersion should be taken. A very good agreement was found between values of film thickness calculated using this method and those measured using Tolansky's approach.

3.2. Refractive index n

Away from absorption, the refractive index n is given by [20]

$$n = [M + (M^2 - s^2)^{1/2}]^{1/2} \text{ ....} (3)$$

where

$$M = \frac{2s}{T_m} - \frac{s^2 + 1}{2}$$

and T_m is the transmission minimum and s is the refractive index of the substrate.
In the region of weak and medium absorption, where the absorption coefficient $\alpha \neq 0$, the refractive index n is given by

$$n = [N + (N^2 - s^2)^{1/2}]^{1/2} \qquad (4)$$

where

$$N = 2s\frac{T_M - T_m}{T_M T_m} + \frac{s^2 + 1}{2}$$

and T_M is the transmission maximum. The spectral envelopes of the transmittance, $T_M(\lambda)$ and $T_m(\lambda)$ (which are assumed to be continuous functions of the wavelength) were computed using a polynomial interpolation between extrema. In the region of strong absorption, n can be estimated by extrapolating the values calculated in the other regions of the spectrum.

3.3. Absorption coefficient α

The absorption coefficient α can be determined if the absorbance x is calculated from the relation

$$x = \exp(-\alpha d) \quad \text{..} (5)$$

In the region of weak and medium absorption, x is given by two different relations. Using the transmission maximum T_M, x is given by

$$x = \frac{E_M - [E_M^2 - (n^2-1)^3(n^2-s^4)]^{1/2}}{(n-1)^3(n-s^2)} \quad \text{....................} (6)$$

where

$$E_M = \frac{8n^2 s}{T_M} + (n^2-1)(n^2-s^2)$$

Using the transmission minimum T_m, x is given by

$$x = \frac{E_m - [E_m^2 - (n^2-1)^3(n^2-s^4)]^{1/2}}{(n-1)^3(n-s^2)} \qquad (6)$$

where

$$E_m = \frac{8n^2 s}{T_m} - (n^2-1)(n^2-s^2)$$

3.4. Extinction coefficient k

When the absorption coefficient α is known, the extinction coefficient k can be found from the relation

$$k = \alpha\lambda / 4\pi \quad \text{..} (7)$$

The real and imaginary parts of dielectric constants ε_1 and ε_2 can be calculated if the refractive index and extinction coefficient are known using the relations $\varepsilon_1 = (n^2 - k^2)$ and $\varepsilon_2 = 2nk$

3.5. Evaluation of material characteristic energies

An interesting model (single oscillator model) describing the index dispersion behavior was proposed by Wemple and Di Domenico [21, 22]. It accounts for the dispersion curve according to the relation

$$n^2(\hbar\omega) = 1 + \frac{E_d E_w}{E_w^{\ 2} - (\hbar\omega)^2} \tag{8}$$

where $\hbar\omega$ is the photon energy, E_w and E_d are two parameters connected to the optical properties of the material and they are known as the single oscillator energy and the oscillator strength respectively. E_w defines the average energy gap usually considered as the energy separation between the centers of both the conduction and the valence bands. E_d is a measure of the average strength of the interband optical transitions. Plotting $(n^2\text{-}1)^{-1}$ against $(\hbar\omega)^2$ and fitting it to the straight part of the curve in the high-energy region allows obtaining from the slope and the intercept values of the single oscillator parameters (E_w and E_d).

3.6. High frequency dielectric constant and carrier concentration

The real part of the complex dielectric constant could expressed as [24]

$$\varepsilon_1 = n^2 - k^2 = \varepsilon_\infty - \frac{e^2}{4\pi^2 c^2 \varepsilon_0} \frac{N}{m^*} \lambda^2, \tag{9}$$

where ε_0 is the free space dielectric constant, N/m^* the ratio of free carrier concentration, N, to the free carrier effective mass, m^*. Plotting of ε_1 versus λ^2 both the high frequency dielectric constant ε_∞ and N/m^* could be determined.

3.7. Urbach energy and tail of absorption edge

It is well known that the shape of the fundamental absorption edge in the exponential (Urbach) region yields information on the disorder effects [25]. With incident photon energy less than the band gap, the increase in absorption coefficient is followed with an exponential decay of density of states of the localized into the gap [26] and the absorption edge is known as Urbach edge. The lack of crystalline long-range order in amorphous/glassy materials is associated with a tailing of density of states [26]. At lower values of the absorption coefficient (1 cm^{-1} < α < 10^4 cm^{-1}), the extent of the exponential tail of the absorption edge characterized by the Urbach energy is given by [27]

$$\alpha(h\nu) = \beta \exp(h\nu/E_U) \tag{10}$$

where β is a constant, E_U is the Urbach energy which indicates the width of the band tails of the localized states. The optical absorption coefficient just below the absorption edge shows exponential variation with photon energy indicating the presence of Urbach's tail. Plotting ln(α) vs. $h\nu$ and taking the reciprocals of the slopes of the linear portion in the lower photon energy of these curves, E_U could be obtained

3.8. Analysis of energy gap

An expression for the absorption coefficient, $\alpha(h\nu)$, as a function of photon energy ($h\nu$) for direct and indirect optical transitions is given by the following expression [28].

$$\alpha(\nu) = \frac{A(h\nu - E_g^{opt})^m}{h\nu} \tag{11}$$

where the exponent m =1/2 for allowed direct transition, while m = 2 for allowed indirect transition. E_g^{opt} is optical band gap energy (Tauc gap) and A is a constant related to the extent of the band tailing. Plotting $(\alpha h\nu)^{1/2}$ against photon energy ($h\nu$) gives a straight line with intercept equal to the optical energy band gap for indirect (E_g^{opt}) transitions. The optical gap can also be found from the imaginary part ε_2 of the dielectric constant [8]. Plotting $(\varepsilon_2)^{1/2}$ versus Photon energy defines the optical gap $E_g^{'}$ from the extrapolated intercept.

4. Results and discussion

The dispersion of the refractive index n for different samples is shown in Fig. (1). The figure shows a normal dispersion behaviour (where $dn/d\lambda$ is negative). From figure, the dispersion curves show an increase with increasing the thickness. Similar observation was previously reported for sputtered samples [8] and those grown by glow discharge [9]. The same behavior was also reported for other amorphous thin films [12, 13]. Values for the refractive index at λ = 850 nm (comparable to λ infinity) is given in Table (1) (error in n is 0.007). It can be seen that, for thickness higher than 490 nm the opposite behavior starts to show, in which a decrease in the refractive index is obtained with the further increase in the film thickness. A similar behavior was reported for sputter deposited Nb_2O_5 films [12]. Figure (2) shows for the Si-1 sample a proof of a direct band gap transition at low energy values. The value for this gap was calculated and found to be 0.52 eV.

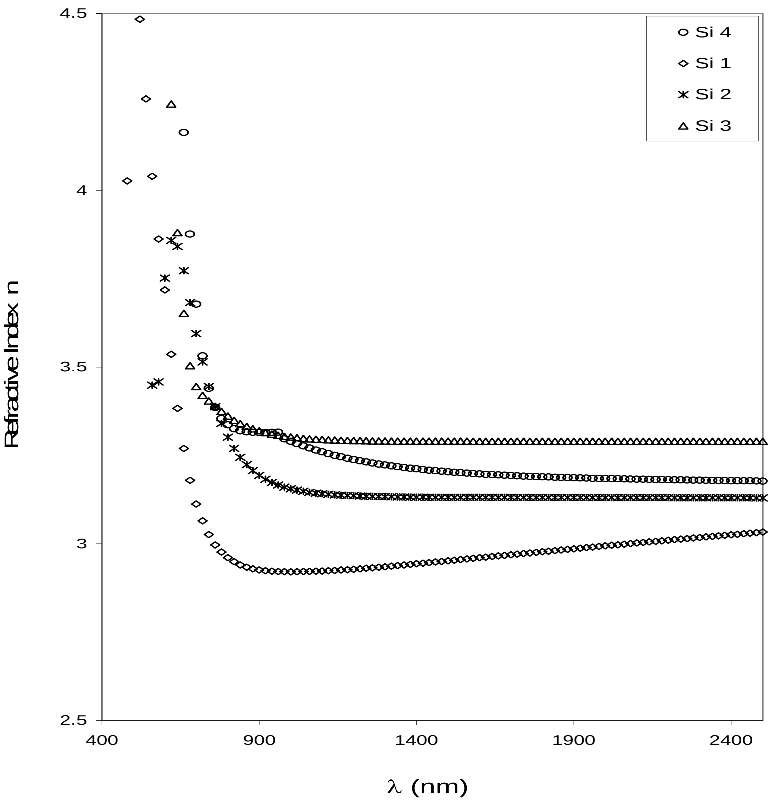

Fig. (1): Variation of the normal dispersion curve of refractive index *n* with film thickness

Table (1): Calculated values of the Tauc optical gap E_g^{opt}, the optical gap calculated using imaginary part of dielectric constant $E_g^{'}$, Urbach parameter E_u, average gap E_w, oscillator strength E_d, carrier concentration N/m^*, refractive index n, high frequency dielectric constant ε_∞ and static refractive index n_o.

Sample	Thickness (nm)	E_g^{opt} (eV)	$E_g^{'}$ (eV)	E_u (meV)	E_w (eV)	E_d (eV)	N/m^* $\times 10^{21}$ (cm^{-3})	n (850 nm)	ε_∞	n_o
Si 1	190	1.8	1.68	265	2.59	12.02	4.42	2.94	8.45	2.36
Si 2	405	1.73	1.65	128	2.61	16.66	9.37	3.14	9.81	2.72
Si 3	490	1.53	1.62	125	2.24	7.88	31.2	3.34	10.84	3.16
Si 4	540	1.56	1.68	176	2.21	9.91	71.0	3.32	10.21	3.22

The absorption coefficient is plotted for different thickness and energy and shown in Fig. (2). It is seen that α is higher for thinner films showing little dependence for thicker films. The absorption edge shifts also to smaller values of energy with increase in thickness. As for thickness greater than 490 nm, it showed similar opposite behavior as in case of refractive index.

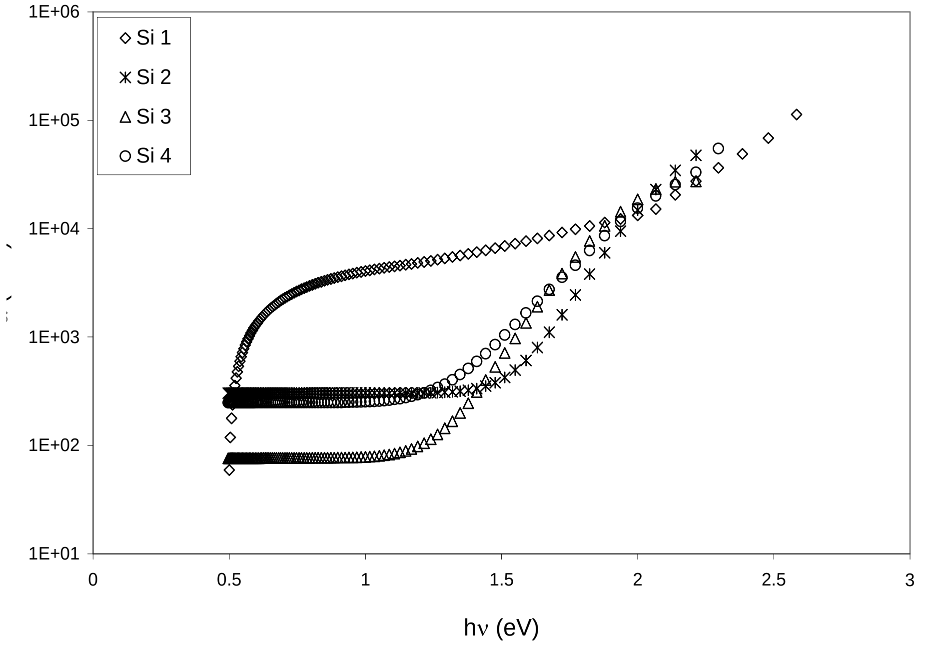

Fig. (2): The change of the absorption coefficient α with film thickness.

The variation of E_g^{opt} and E_g' with thickness is shown in Figs. (3 and 4). Values of E_g^{opt} and E_g' are given in Table 1 (error is 0.01). It can be seen that E_g^{opt} decreases with increasing thickness (same as reported by Demichelis *et al*. [8] and Talukder *et al*. [11]), reaching a saturation value for thickness 490 nm. The opposite behavior was previously reported [9] but with critical thickness of 0.9 μm. The decrease of E_g^{opt} with thickness was interpreted by Talukder *et al*. [11] as due to the fact that the surface layers of the film can vary in a fundamental way from the bulk layer. This is owing to an unintentional grading of the constituents of the material. However, values of E_g' showed no significant change with thickness. Demichelis *et al*. [8] and Cody *et al*. [29] reported the same conclusion and related this behavior to the non-direct type of optical transitions in amorphous materials. In non-direct optical transitions the electron momentum is no longer a good quantum number, so that the assumption of a constant momentum matrix element, leading to E_g^{opt}, seems to be incorrect. The assumption of a constant dipole matrix element, which is more general and free of momentum constraints, leads to $E_g^{'}$.

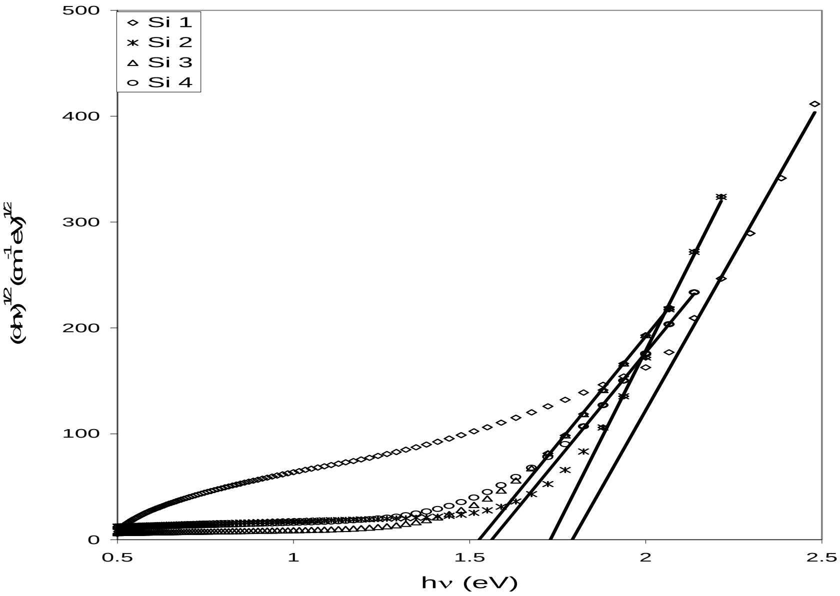

Fig. (3): Plots of the optical gap as calculated from Tauc's equation for different film thicknesses.

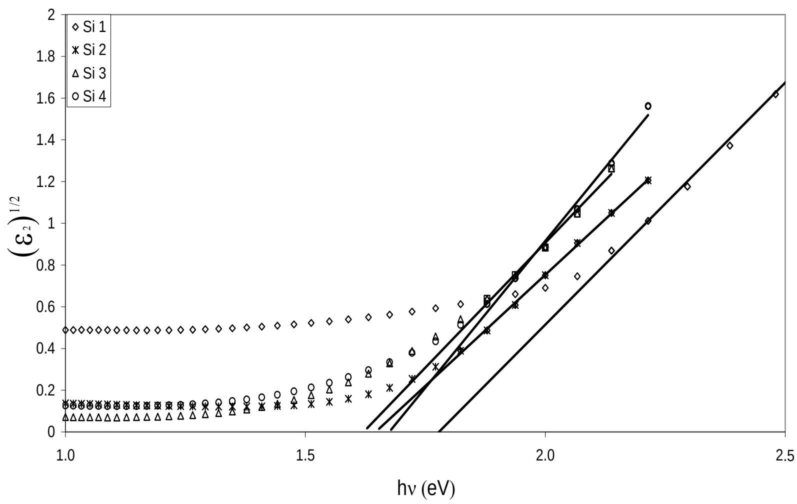

Fig. (4): Plots of the optical gap as calculated from using the imaginary part of dielectric constant for different film thicknesses.

Values of the Urbach parameter E_u are listed in Table (1). As shown in table, E_u decreased with increase in film thickness for values less than 490 nm. As the Urbach parameter is a measure of the degree of disorder, the assumption of the presence of defects in the thinly amorphous film seems to be valid in our case. During the deposition of amorphous film, unsaturated bonds are produced as a result of insufficient number of atoms. The unsaturated bonds are responsible for the formation of some defects in the film. Such defects produce localized states. In the case of thicker films, greater deposition builds up a more homogeneous network. Calculated values of E_w and E_d are given in Table (1). The results show that values of the average gap agreed in behavior with the calculated Tauc gap (E_g^{opt}), i.e., decreased with increasing film thickness.

The change in the carrier concentration is calculated and given in Table (1). The data in table shows that the carrier concentration increases with increasing film thickness, such increase could be explained as follows [9]. Tetrahedral amorphous semiconductor thin films exhibit inhomogeneities. For thicker films, longer deposition time builds up better homogeneity with better compensation of dangling bonds. Poor compensation of dangling bonds and inhomogeneities which are predominant at the substrate-film interface dominates over the bulk since the surface to volume ratio is higher for thinner films. Since thicker films are more homogeneous, and also the surface to volume ratio is lower than that of thinner films, the influence of the interface and surface to bulk becomes less crucial. Hence, the disorder induced tailing decreases for thicker films. This decrease is due to the lower density of defects and better homogeneity which reduces the density of localized states near the mobility edges, and thereby reducing the extent of tailing. So the donor type defect states, below E_f, which otherwise had been occupied in the thinner films, becomes neutral, releasing electrons. These electrons can be accepted by the acceptor type defect states above the Fermi level and go to the conduction band. When it is accepted by the defect states above the Fermi level, the defect state is negatively charged and hence has to be below the Fermi level. Hence the Fermi level rises, and when it reaching the conduction band, the carrier concentration increases.

Values of the static refractive index n_o are calculated and given in Table (1). n_o increased with increasing thickness. The static refractive index n_o is the lower limit of refractive index and it represents the response of the material to DC electric field and it is proportional to the carrier concentration N. It is given by [28],

$$n_o^2 \propto \frac{Ne^2}{\varepsilon_o m \omega_o^2} \tag{12}$$

From the above equation it is clear that n_o depends on the carrier concentration, *N*, where *e* and *m* are the charge and mass of the electron, respectively. ε_o is the permittivity of vacuum and ω_o is the oscillator natural frequency. Consequently, with the increase carrier concentration *N*, n_o shows an increase as listed in Table (1).

The calculated values for the high frequency dielectric constant ε_∞ are listed in Table (1). As could be seen that ε_∞ increased with film thickness up to 490 nm, *i.e.*, increased with increasing saturation of dangling bonds. Beyond this thickness, ε_∞ started to decrease.

5. Conclusion

Investigations of the dependence of optical constants on film thickness of vacuum-deposited hydrogenated amorphous silicon thin films are reported in the present study. The refractive index dispersion curves shifted to higher values with increasing the thickness. The absorption coefficient α is higher for thinner films and showed little dependence for thicker films. The optical gap E_g^{opt} (Tauc gap) decreases with increasing thickness, reaching a saturation value for thickness 490 nm. Values of optical gap calculated using imaginary part of dielectric constan $E_g^{'}$ showed no significant change with thickness. Values of the Urbach parameter E_u decreased with the increase in film thickness for values less than 490 nm. Values of the average gap, calculated using Wemple's equation, E_w agreed in behavior with that calculated using Tauc's equation, i.e., decreased with increasing film thickness. The carrier concentration increased with film thickness. Values of the static refractive index n_o increased with increasing thickness. The high frequency dielectric constant ε_∞ increased with thickness up to 490 nm. Beyond this thickness, ε_∞ started to decrease

References

1. A. M. Bakry and A. H. El-Naggar, *Thin Solid Films*, **360**, 293 (2000).
2. A. H. El-Naggar and A. M. Bakry, *Journal of Physics: Condensed Matter*, **11**, 9619 (1999).
3. C. C. Rsai and H. Fritzshe, *Sol. Energy Mater.*, **1**, 11 (1979).
4. G. Myburg and R. Swanepoel, *J. Non-Cryst. Solids*, **89**, 13 (1987).
5. G. D. Cody, B. Abeles, C. R. Wronski, R. B. Stephens and B. Brooks, *Solar Cells*, **2**, 227 (1980).

6. T. J. Kamino and T. R. Cass, *Thin Solid. Films*, **16**, 147 (1973).
7. R. M. Anderson, *J. Electrochem. Soc*., **120**, 1540 (1973).
8. F. Demichelis, G. Kanidakis, E. Mezzetti, P. Mpawenayo, A. Tagliaferro, E. Tresso, P. Rava and G. Della, *Thin Solid Films*, **150**, 1 (1987).
9. R. Sridhar, R. Venkattasubbiah, J. Mahjhi and R. Ramachandran, *J. non-cryst. Solids*, **119**, 331 (1990).
10. H. V. Nguyen, S. Kim, Y. M. Wakagi and R. W. Collins, *J. non-cryst. Solids*, **198**-**200**, 853 (1996).
11. G. Talukder, J. A. Cowan, D. E. Brodie and J. D. Leslie, *Can. J. Phys*., **62**, 848 (1984).
12. F. Lai, L. Lin, Z. Huang, Gai and Y. Qu, *Appl. Surf. Sci*., **253**, 1801 (2006).
13. S. Velumani, X. Mathew, P. J. Sebastian, Sa. K. Narayandass and D. Mangalaraj, *Sol. Energy mat. And sol. Cells*, **76**, 347 (2003).
14. E. Abd El-Wahabb, M. M. El-Samanoudy and M. Fadel, *Appl. Surf. Sci*., **174**, 106 (2001).
15. S. K. Biswas, S. Chaudhuri and A. Choudhury, *phys. stat. sol. (a)*, **105** 467 (1988).
16. M. A. Abdel-Rahim, *J. Phys. And Chem. Solids*, 60 29 (1999).
17. A. A. Abu-Sehly and M. I. Abd-Elrahman, *J. Phys. And Chem. Solids*, **63** 163 (2002).
18. S. Tolansky, "*Multiple-Beam Interference.Microscopy of Metals*", Academic, London, p.55 (1970).
19. M. Ambrico, *Semicond. Sci. Technol*. **13**, 1446 (1998).
20. R. .Swanepoel, *J. Phys. E : Sci. Instrum*., **16**, 1214 (1983).
21. S. H. Wemple, M. Di Domenico, *Phys. Rev*., **B3**, 1338 (1971).
22. S. H. Wemple, *Phys. Rev*., **B7**, 3767 (1973).
23. M. Abdel-Baki, F. A. Abdel Wahab, F. El-Diasty, *Mater. Chem. Phys*. **96**, 201 (2006).
24. T. S. Moss, G. J. Burrell and E. Ellis, *Semiconductor Opto-Electronics*, Butterworths, London, (1973).
25. G.D. Cody, T. Tiedje, B. Abeles, B. Brooks, Y. Goldstein, *Phys. Rev. Lett*., **47**, 1480 (1981).
26. B. Abay, H. S. Guder, Y. K. Yogurtchu, *Solid State. Commun*., **112**, 489 (1999).
27. M. A. Hassan, C. A. Hogarth, *J. Mater. Sci*., **23**, 2500 (1988).
28. E. A. Davis, N. F. Mott, *Phil Mag*., **22,** 903 (1970).
29. G. D. Cody, B. G. Brooks and B. Abeles, *Sol. Energy Mater*., **8,** 231 (1982).
30. M. Fox, "*Optical Properties of Solids"*, Oxford, p.32 (2003).